8. P. Racz, K. Tenner, E. Mérö, *Lab. Invest.* **26**, 694 (1972).
9. Supplementary data and information on experimental protocols are available on *Science* Online at www.sciencemag.org/cgi/content/full/292/5522/1722/DC1.
10. M. Lecuit and P. Cossart, unpublished data.
11. The −1178 +28 rat *iFABP* promoter sequence was amplified and subcloned in-frame and upstream of *hEcad* cDNA in pSK-(hEcad) (7). The human β-globin intron 2 and a polyadenylate tract was placed downstream of *hEcad* to improve transcriptional efficiency in transgenic mice. The purified 5545–base pair DNA construct was microinjected in (C57BL/6J × SJL/J)$F_2$ zygotes and reimplanted in pseudopregnant (C57BL/6J × CBA/J)$F_1$ mice (9).
12. M. L. Hermiston, M. H. Wong, J. I. Gordon, *Genes Dev.* **10**, 985 (1996).
13. B. Pron *et al.*, *Infect. Immun.* **66**, 747 (1998).
14. P. Cossart, M. Lecuit, *EMBO J.* **17**, 3797 (1998).
15. T. M. Mayhew, R. Myklebust, A. Whybrow, R. Jenkins, *Histol. Histopathol.* **14**, 257 (1999).
16. S. Dramsi *et al.*, *Mol. Microbiol.* **16**, 251 (1995).
17. Y. Shen, M. Naujokas, M. Park, K. Ireton, *Cell* **103**, 501 (2000).
18. C. Birchmeier, E. Gherardi, *Trends Cell Biol.* **8**, 404 (1998).
19. A. Marra, R. R. Isberg, *Infect. Immun.* **65**, 3412 (1997).
20. R. Schulte *et al.*, *Cell. Microbiol.* **2**, 173 (2000).
21. D. Figarella-Branger *et al.*, *Acta Neuropathol.* **89**, 248 (1995).
22. L. L. Rubin *et al.*, *J. Cell Biol.* **115**, 1725 (1991).
23. Y. Shimoyama *et al.*, *Cancer Res.* **49**, 2128 (1989).
24. R. B. Ren, F. Constantini, E. J. Gorgacz, J. J. Lee, V. R. Racaniello, *Cell* **63**, 353 (1990).
25. M. B. A. Oldstone *et al.*, *Cell* **98**, 629 (1999).
26. We thank M. Takeichi for the gift of HECD1 hybridoma; J. I. Gordon for rat *iFABP* promoter DNA; V. R. Racaniello for human β-globin intron 2 DNA; H. Khun for the immunolabeling of tissue sections; and S. Dramsi, G. Milon, and H. Ohayon for help in preliminary experiments. These studies were supported by Association de Recherche sur le Cancer, the European Economic Commission, Ministère de l'Education Nationale, de l'Enseignement Supérieur et de la Recherche, CNRS, and Institut Pasteur. P.C. is an international investigator from the Howard Hughes Medical Institute.

14 February 2001; accepted 24 April 2001

# Structure of Complement Receptor 2 in Complex with Its C3d Ligand

**Gerda Szakonyi,[1]* Joel M. Guthridge,[2]* Dawei Li,[1] Kendra Young,[2] V. Michael Holers,[2] Xiaojiang S. Chen[1]†**

**Complement receptor 2 (CR2/CD21) is an important receptor that amplifies B lymphocyte activation by bridging the innate and adaptive immune systems. CR2 ligands include complement C3d and Epstein-Barr virus glycoprotein 350/220. We describe the x-ray structure of this CR2 domain in complex with C3d at 2.0 angstroms. The structure reveals extensive main chain interactions between C3d and only one short consensus repeat (SCR) of CR2 and substantial SCR side-side packing. These results provide a detailed understanding of receptor-ligand interactions in this protein family and reveal potential target sites for molecular drug design.**

Complement receptor type 2 (CR2 or CD21), the receptor for complement component C3d, is a key interface between innate and adaptive immunity (*1*). C3d attaches to foreign antigens (such as invading microorganisms) (*2*) and these C3d-bound antigens amplify B cell responses by simultaneously binding to CR2 through C3d and to the B cell receptor (BCR) via the bound antigen (*3*). The cross-linking of CR2 to the BCR amplifies a signal transduction cascade through the CR2/CD19/CD81 co-activation complex (*1*). CR2 mediates the interaction of C3-bound HIV-1 as an immune complex with B cells and so promotes transfer of virus and infection of CD4 T cells (*4*). Human CR2 is also a receptor for CD23 (*5*) and is the obligate receptor for the Epstein-Barr virus (EBV) (*6*). In addition, CR2 is essential for the development of normal humoral immunity to T-dependent antigens (*7–9*) and has been implicated in the maintenance of B cell self-tolerance and the development of autoimmunity (*10*).

Interactions with all three human CR2 ligands require the first two of 15 or 16 short consensus repeats (SCR1 and SCR2) of CR2 (*11*, *12*). SCR domains, like immunoglobulin domains, are found in many proteins from both complement and non-complement families and mediate diverse biological functions (*13*). SCR domains have a conserved core structure but variable orientations between domains mediated in part by relatively short three to eight amino acid inter-SCR linker peptides (*14–16*). At least two SCR domains are required to mediate protein-protein interaction, and the relative angle and orientation between domains is likely to contribute to biologic diversity and specificity. The lack of a high-resolution structure of a receptor-ligand complex in this family has hindered our understanding of the molecular recognition mechanisms of this class of proteins. To gain insight into CR2 interactions, we have determined the crystal structure of the CR2 SCR1 and SCR2 domain in complex with C3d at 2.0 Å (*17*).

The complex contains a V-shaped CR2 receptor binding to a globular C3d ligand (Fig. 1A and Table 1). The V-shaped CR2

**Table 1.** Structure determination and refinement. ASU, assymetric unit; rmsd, root mean square deviation.

| | |
|---|---|
| *Data collection statistics* | |
| Space group | R32 |
| Unit cell length (Å) | $a = b = 170.5$, $c = 173.8$ |
| Molecules/ASU | 3 |
| Resolution (Å) | 25.0–2.04 |
| Completeness (last bin) | 94.1 (83.6) |
| Total reflections | 255801 |
| Unique reflections | 65612 |
| $R_{sym}$ (last bin)%* | 6.7 (22.3) |
| $I/\sigma$ (last bin) | 10.8 (3.7) |
| *Refinement statistics* | |
| % of reflections for $R_{free}$ | 10 |
| $R_{work}/R_{free}$ | 20.8/23.9 |
| Rmsd from ideality | |
| Bond length (Å) | 0.006 |
| Bond angle (°) | 1.10 |
| Dihedral angle (°) | 16.8 |
| Ramachandran plot (core, disallowed) | 92.3 (0) |
| Average B factor | 33.98 |
| Rmsd of B factor (Å$^2$) | 1.2 |
| Protein atoms in the model | 8878 |
| $H_2O$ in the model | 580 |

*$R_{sym} = \Sigma_{ij} |I(j) - \langle I(j)\rangle| / \Sigma_{ij} I_i(j)$, where $I_i(j)$ is the $i$th measurement of reflection $j$, and $\langle I(j)\rangle$ is the overall weighted mean of $j$ measurements.

[1]Department of Biochemistry and Molecular Genetics, [2]Departments of Medicine and Immunology, University of Colorado Health Science Center, School of Medicine, Denver, CO 80262, USA.

*These authors contributed equally to this work.
†To whom correspondence should be addressed. E-mail: Xiaojiang.Chen@uchsc.edu

molecule has a span of 42.6 Å at the base, and the height of the "V" structure measures 38.5 Å. The C3d ligand, which has a dome-shaped helical structure (*18*), interacts with the receptor using one portion of the edge of the dome. Because the CR2-contact edge of C3d is located nearly opposite the amino ($NH_2$) and carboxyl (COOH) termini, binding to CR2 will likely orient the rest of the iC3b form of C3, a larger molecule that contains the C3d domain and also binds CR2, away from the interaction site. The site of the ester-bond linkage to antigens (Q20) (*19*) is approximately halfway between the receptor contact edge and the $NH_2$- and COOH-termini of C3d.

The CR2 structure here contains the first 134 residues following the signal peptide that fold into two SCR domains (Fig. 2A). Each domain has the characteristic SCR β barrel structure (*13–16*). An *N*-acetyl-glucosamine residue is attached to N102 (*19*). An eight–amino acid linker, the longest found so far in this family, bends to allow the two SCR domains to pack against each other sideways. Available structures of four other SCR proteins containing two or four repeats all have end-end packing between consecutive SCRs (*13–16*). Thus, CR2 is the first to demonstrate extensive side-side packing. The interface between the two domains is mainly hydrophobic (Fig. 2B). W112, which is unique to CR2 SCR2 sequence and is located on strand D2, plays a critical role in the packing by interacting with L38 and I39 and the main chain from SCR1. P121, H91, and the carbon side chain of E64 also participate in the interface. The linker, which contains mainly hydrophobic residues (Y65, F66, and Y69), participates in the hydrophobic packing outside the two-domain interface, further solidifying the interactions between SCR1 and SCR2. Unlike end-end packing, this packing does not allow rotation of the domains relative to each other about the interface (*14*, *15*).

Two CR2 molecules dimerize through SCR1-SCR1 contacts in the crystal structure (*20*). The contact is symmetrical, with the E1 strands from different molecules running anti-parallel to each other and the COOH-terminus of the E1 strand also contacting the COOH-terminus of the D2 strand of another molecule. The interaction is through hydrogen bonds (H-bonds). This interaction may exist only in the crystal contact as CR2 behaves as a monomer in solution. However, it is also possible that the dimerization may be physiologically relevant in the cell membrane.

The CR2-C3d interface demonstrates a striking shape complementarity with a total buried surface area of 1400 $Å^2$ (Fig. 3, A and B). No major conformational difference is observed between the structures of free C3d and CR2-bound C3d, except for small movements (0.7 to 1.0 Å) of H3 (helix 3), H5, H7, and a few turns or loops on the surface.

Residues that are separated in the linear sequence but come together in folded C3d participate in the interaction interface. In particular, residues on the H3-H4 loop, H5, and H7 contact CR2 (Fig. 3C). From CR2, a linear stretch of residues within the B strand and B-C loop of SCR2 constitute the majority of the interactions with C3d through networks of H-bonds together with hydrophobic and van der Waals interactions (Fig. 3, D and E). Well-ordered water molecules participate in the formation of some H-bonds between CR2 and C3d. It is intriguing that only SCR2 directly contacts C3d because previous studies have shown that both SCR1 and SCR2 are required for binding of polymeric forms of C3d to CR2 on cell membranes (*11*, *12*, *21*). The requirement for both domains to bind C3d on the cell surface indicates that inter-SCR packing is necessary for stabilization of the SCR2 site.

An interesting feature of the CR2-C3d interaction is the extensive use of main-chain atoms in forming H-bonds between CR2 and C3d. In particular, in C3d most of the H-bond contributors come from main-chain carbonyl groups (Fig. 3, D and E) and no side chains other than N170 are involved in direct interactions with CR2 (*20*). This observation likely explains the previous difficulties in accurately identifying the residues that directly interact with CR2, either by site-directed mutagenesis of C3d or by using C3d-derived inhibitory peptides (*22*). This interaction mode of CR2-C3d is reminiscent of major histocompatibility complex (MHC)–antigen peptide recognition, where MHC interacts with the main-chain atoms of the antigen peptide to allow binding to a range of peptides (*23*). In the CR2-C3d interaction, specificity is maintained because of the extensive shape complementarity.

At the COOH-terminal end of H5 the carbonyl groups from I115, L116, E117, and Q119 of C3d form an anion hole (Fig. 3D) that is occupied by the positively charged R84 of CR2. Here, R84 acts as an in-trans capping residue to seal the α helical dipole moment at the COOH-terminus of H5 of C3d. The more usual interaction involving an α helical dipole moment is when a negatively

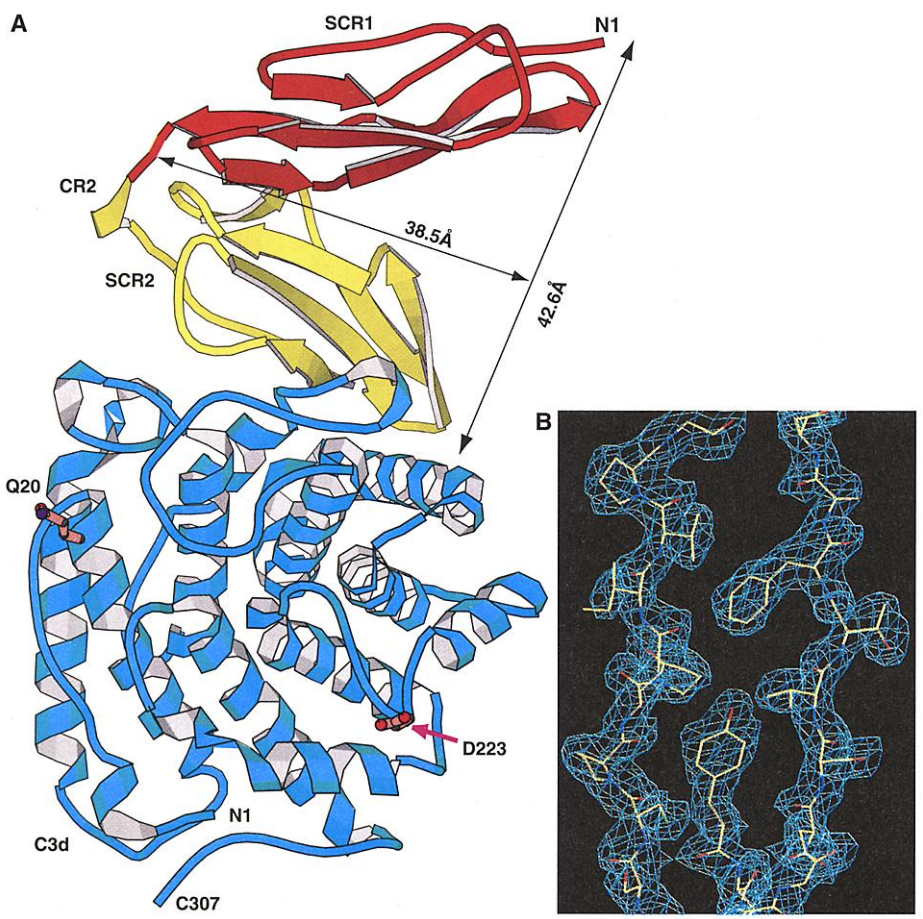


**Fig. 1.** Structure of the CR2-C3d complex. (**A**) Overall view of the structure of CR2 binding to C3d. CR2 SCR1 is in red, SCR2 in yellow, and C3d in cyan. Residue Q20 of C3d that forms an ester-bond with antigen is drawn in pink and labeled. Residue D223 of C3d in the C3F form, which is associated with an increased incidence of certain immune diseases (*32*), is also labeled (prepared using MOLSCRIPT). (**B**) Part of CR2 electron density showing clear features of amino acid side chains.

charged group from one protein interacts with the positively charged $NH_2$-terminus of a helix in its interaction partner (*24*).

The conformation of the C3d-binding region, the B-C loop of SCR2 domain on CR2, is important for positioning R84 (Fig. 3, C, D, and E). G85 does not sterically interfere with the CR2 and C3d interface interaction, and the side chain of S86 forms an H-bond with a carbonyl oxygen from the H3-H4 loop of C3d through a water molecule (Fig. 3, D and E). Other residues around R84 have side chains pointing away from the interface and use their main-chain atoms to form H-bonds with C3d. It is likely that the basic capping residue R84, as well as S86, is critical to the interaction.

Mutagenesis of C3d around the interface to disrupt CR2 binding provide support for CR2-C3d interaction seen (Fig. 4). Specifically, in a CR2-binding inhibition assay, two C3d mutants involving the N170 residue [mut2 with N170R ($Asn^{170} \rightarrow Arg^{170}$) or mut4 with N170A, I115R, and L116R] did not effectively inhibit the interaction of CR2 with wild-type C3d. In contrast, a mutant (mut1 with L116A or E117A) involving residues where only main-chain interactions are seen still strongly interacted with CR2.

Previous studies have demonstrated a substantial salt dependence for CR2-C3d binding in a similar fashion to other C3/C4 receptor: ligand interactions. For the interactions in the CR2-C3d complex, the set of H-bonds formed through the charged R84 of CR2 belongs to the class of strong H-bonds that are similar to salt bridges. Thus, these H-bonds, which constitute the center of the interface, are expected to be strongly influenced by salt concentration. In addition, the H-bonds mediated through the charged K100 of CR2 and K178 of C3d (Fig. 3E) should be sensitive to salt concentration.

On the basis of the structure of the CR2-C3d complex, we can now explain the results from previously reported CR2 peptide inhibition and monoclonal antibody assays (*25*–*27*). CR2-derived peptides from the B strand of SCR1 as well as the B strand and B-C loop of SCR2 inhibited CR2-C3d interaction (*26*). The SCR2 peptides are from within the interaction interface seen in the complex (Fig. 3, D and E). We suggest that the inhibition caused by the SCR1 peptides is due to structural similarity to the SCR2 peptides. Previously mapped epitope positions on CR2 for inhibitory monoclonal antibodies also support the interaction sites seen in the CR2-C3d complex structure (*20*). Two inhibitory antibodies, OKB7 (*25*) and FE8 (*27*), have epitopes positioned next to the C3d binding region. We have also created additional monoclonal antibodies that inhibit the specific binding of CR2 to C3d (*20*). All have mapped epitopes on CR2 that are within or adjacent to the C3d-interacting area. Previous

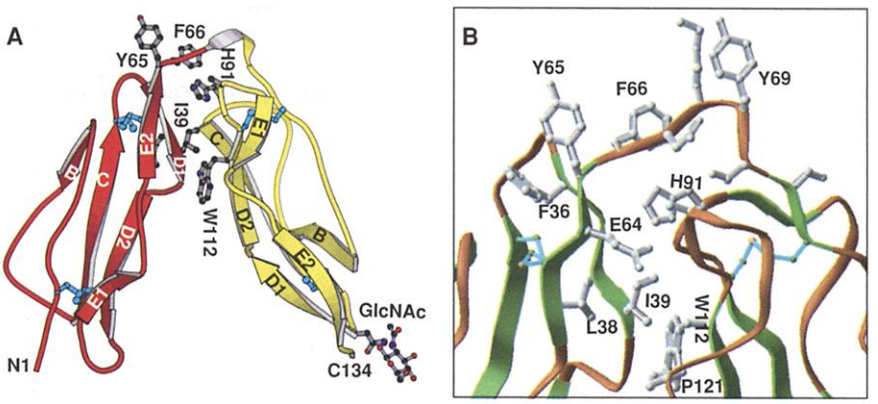


**Fig. 2.** Structure of CR2. (**A**) Ribbon representation of the CR2 SCR1 (red) and SCR2 (yellow) structures, showing the SCR fold and the packing of the two domains to form a V shape. The intra-domain disulfide bonds are in cyan. (**B**) The structure and packing interaction at the interface of SCR1 and SCR2 domains. Residues important for the tight packing between the two domains at the interface and the linker regions are shown (prepared using RIBBONS).

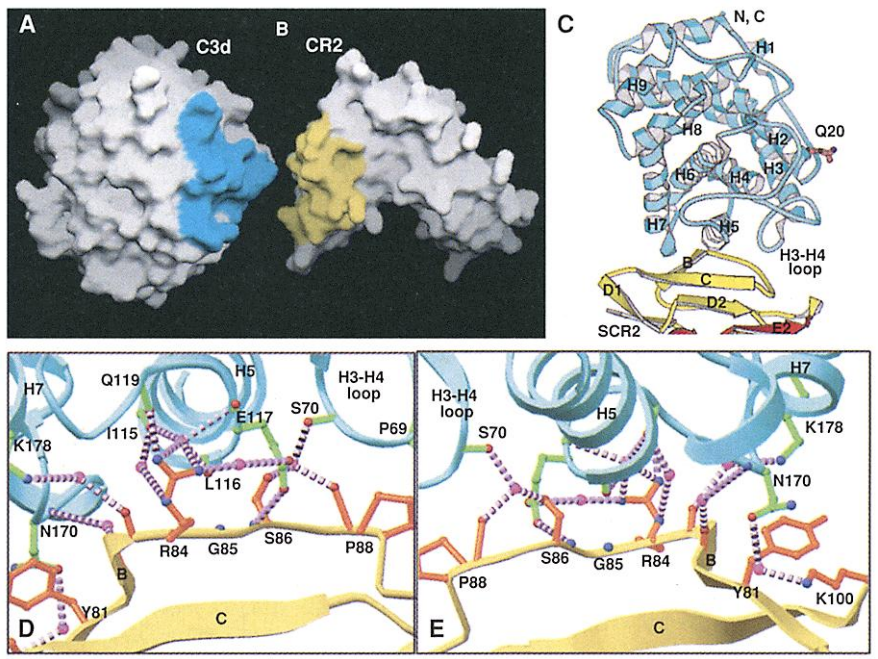


**Fig. 3.** Structure at the CR2-C3d interface. (**A** and **B**) Surface features of the interface area on C3d (in cyan) and CR2 molecule (in yellow). The shape of the interface of one molecule complements that of the other (prepared using GRASP). (**C**) Structure of the CR2 SCR2 (yellow) and C3d (cyan) complex. (**D** and **E**) The detailed interactions between CR2 (yellow) and C3d (cyan) in two angles. Dashed lines represent H-bonds between carbonyl oxygen atoms (red), nitrogen atoms (blue) of amino acid side chains or main chain, and water molecules (pink).

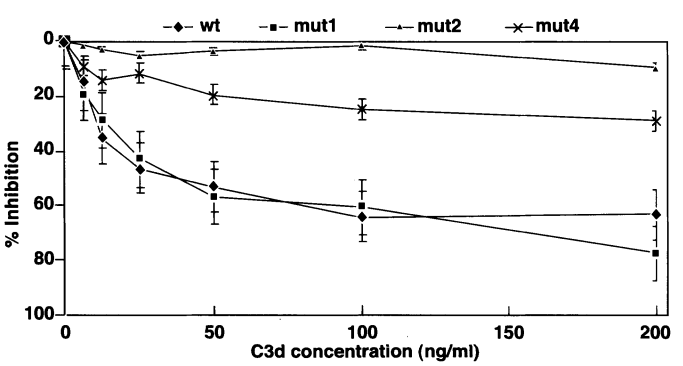


**Fig. 4.** ELISA results demonstrating the relative inhibition of binding of full-length soluble CR2 at 2 μg/ml to plate-bound C3d by wild-type C3d (wt) compared to mutant C3d (mut1, mut2, and mut4) at several concentrations. Wt and mut1 inhibited CR2-C3d binding similarly, whereas mut2 and mut4 have lost most of their inhibitory capabilities and, thus, do not effectively interact with CR2.

evidence suggests that CR2 binds to C3d and EBV gp350/220 with overlapping but distinct sites (*28*) and involves S16 and Y68. These residues mapped on the CR2 surface are separated from the area that interacts with C3d in our complex structure.

### References and Notes


1. D. T. Fearon, *Semin. Immunol.* **10**, 355 (1998).
2. S. K. A. Law, K. B. M. Reid, *Complement*, in *Focus Series*, D. Male, Ed. (IRL Press, Oxford, UK, ed. 2, 1995).
3. R. H. Carter, D. T. Fearon, *Science* **256**, 105 (1992).
4. S. Moir *et al.*, *J. Exp. Med.* **192**, 637 (2000).
5. J. P. Aubry, S. Pochon, P. Graber, K. U. Jansen, J. Y. Bonnefoy, *Nature* **358**, 505 (1992).
6. J. D. Fingeroth, *et al.*, *Proc. Natl. Acad. Sci. U.S.A.* **81**, 4510 (1984).
7. T. Hebell, J. M. Ahearn, D. T. Fearon, *Science* **254**, 102 (1991).
8. J. M. Ahearn *et al.*, *Immunity* **4**, 251 (1996).
9. H. Molina *et al.*, *Proc. Natl. Acad. Sci. U.S.A.* **93**, 3357 (1996).
10. A. P. Prodeus *et al.*, *Immunity* **9**, 721 (1998).
11. C. A. Lowell *et al.*, *J. Exp. Med.* **170**, 1931 (1989).
12. J. C. Carel, B. L. Myones, B. Frazier, V. M. Holers, *J. Biol. Chem.* **265**, 12293 (1990).
13. A. P. Wiles *et al.*, *J. Mol. Biol.* **272**, 253 (1997).
14. P. N. Barlow *et al.*, *J. Mol. Biol.* **232**, 268 (1993).
15. J. M. Casasnovas, M. Larvie, T. Stehle, *EMBO J.* **18**, 2911 (1999).
16. R. Schwarzenbacher *et al.*, *EMBO J.* **18**, 6228 (1999).
17. CR2 SCR1-2 (residues 20–153) and C3d (residues 995–1303) were expressed in *Pichia pastoris* and in *Escherichia coli*, respectively, and were purified to homogeneity as described in (*29*). Briefly, cells expressing CR2 SCR1-2 were lysed by sonication in 10 mM formate (pH 4.0) buffer, and the supernatant was passed over a SP-Sepharose column (SP HiTrap, Amersham Pharmacia Biotech, Uppsala, Sweden). Eluted CR2 was deglycosylated overnight at 37°C with 33,000 units EndoH per milliliter. The deglycosylated sample was passed over SP-Sepharose again, and a 0.0 to 0.5 M NaCl gradient was used to elute the deglycosylated CR2. C3d was purified from *E. coli* cell lysates using a DEAE column, followed by a MonoQ and then a MonoS column. The interactions of the recombinant CR2 and C3d were studied by Biacore, enzyme-linked immunosorbence assay (ELISA), and analytical ultracentrifugation approaches to confirm the specific binding (*29*). The purified CR2 and C3d were co-crystallized using the method of hanging drop by mixing CR2 and C3d at a molar ratio of approximately 1:1, as determined by careful titration of the two components using native gel shift assay. The total protein concentration (CR2 plus C3d) used for setting up the crystallization drops was approximately 20 mg/ml. The crystallization buffer contained 17% polyethylene glycol (PEG) 2K, 0.2 M zinc acetate, and 0.1 M sodium cacodylate (pH 7.36). Synchrotron data were collected from the crystals at BNL and was processed using D*trek (MSC Inc., Woodlands, TX) (Table 1). The space group is R32, with unit cell $a = b = 170.5$Å, $c = 173.8$ Å. AmoRe (*30*) was used to do molecular replacement that was carried out using C3d (Protein Data Base accession number 1C3D) as a search model. Initial phase improvement was carried out using solvent flattening by the program DM (*30*). Stepwise model building and refinement were carried out using program "O" and CNS (*31*). The final complete model was refined using simulated annealing, positional refinement, and individual B factor refinement. Water molecules were added last using CNS.
18. B. Nagar, R. G. Jones, R. J. Diefenbach, D. E. Isenman, J. M. Rini, *Science* **280**, 1277 (1998).
19. Single-letter abbreviations for the amino acid residues are as follows: A, Ala; C, Cys; D, Asp; E, Glu; F, Phe; G, Gly; H, His; I, Ile; K, Lys; L, Leu; M, Met; N, Asn; P, Pro; Q, Gln; R, Arg; S, Ser; T, Thr; V, Val; W, Trp; and Y, Tyr.
20. Web figure 1 is available at *Science* Online at www.sciencemag.org/cgi/content/full/292/5522/1725/DC1.
21. K. R. Kalli, J. M. Ahearn, D. T. Fearon, *J. Immunol.* **147**, 590 (1991).
22. L. Clemenza, D. E. Isenman, *J. Immunol.* **165**, 3839 (2000).
23. P. J. Bjorkman *et al.*, *Nature* **329**, 512 (1987).
24. C. Branden, J. Tooze, *Introduction to Protein Structure* (Gerland, New York, ed. 2, 1999), p. 16.
25. P. E. Rao, S. D. Wright, E. F. Westberg, G. Goldstein, *Cell. Immunol.* **93**, 549 (1985).
26. H. Molina *et al.*, *J. Immunol.* **154**, 5426 (1995).
27. W. M. Prodinger *et al.*, *J. Immunol.* **161**, 4604 (1998).
28. D. R. Martin, R. L. Marlowe, J. M. Ahearn, *J. Virol.* **68**, 4716 (1994).
29. J. M. Guthridge *et al.*, *Biochemistry*, in press.
30. CCP4, *Acta Crystallogr.* **D50**, 760 (1994).
31. A. T. Brunger *et al.*, *Acta Crystallogr.* **D54**, 905 (1998).



32. M. C. Poznansky, P. M. Clissold, P. J. Lachmann, *J. Immunol.* **143**, 1254 (1989).
33. Supported by Cancer League of Colorado and University of Colorado Cancer Center grants to X.C., NIH R0-1 CA53615 to M.H., and x-ray core facility in the Program in Biomolecular Structure at UCHSC. We thank C. Ogata at X4a and M. Becker at X25 at BNL for assistance in data collection and D. Bain, M. Overduin, L. Chen, S. Perkins, and J. Hannan for discussions. CR2 domain PDB accession number 1GHQ.

18 January 2001; accepted 26 April 2001


# Insulin Resistance and a Diabetes Mellitus–Like Syndrome in Mice Lacking the Protein Kinase Akt2 (PKBβ)


**Han Cho,[1] James Mu,[2,6] Jason K. Kim,[6,7] Joanne L. Thorvaldsen,[3,6] Qingwei Chu,[2,6] E. Bryan Crenshaw III,[4] Klaus H. Kaestner,[5] Marisa S. Bartolomei,[3,6] Gerald I. Shulman,[6,7] Morris J. Birnbaum[2,6]***



**Glucose homeostasis depends on insulin responsiveness in target tissues, most importantly, muscle and liver. The critical initial steps in insulin action include phosphorylation of scaffolding proteins and activation of phosphatidylinositol 3-kinase. These early events lead to activation of the serine-threonine protein kinase Akt, also known as protein kinase B. We show that mice deficient in Akt2 are impaired in the ability of insulin to lower blood glucose because of defects in the action of the hormone on liver and skeletal muscle. These data establish *Akt2* as an essential gene in the maintenance of normal glucose homeostasis.**


Type 2 diabetes mellitus is a complex, multisystem disease with a pathophysiology that includes defects in insulin-stimulated peripheral glucose disposal and suppression of hepatic glucose production, as well as in insulin secretion (*1*). Investigations into the molecular pathways that mediate each of these responses in normal individuals has led to the identification of numerous putative signaling molecules, but only a few have been confirmed in vivo as critical to normal glucose homeostasis (*2*). In particular, the in vivo data in support of the insulin receptor, insulin receptor substrate 1 (IRS1) and IRS2, as important to the maintenance of normal insulin responsiveness, have not been matched by equivalent evidence for a physiological role for downstream signaling molecules (*3–6*). The phosphoinositide-dependent serine-threonine protein kinase Akt (also known as protein kinase B, or PKB) has been proposed to be an intermediate in the signaling pathway by which insulin controls both muscle and fat cell glucose uptake as well as hepatic gluconeogenesis (*7–10*). However, experimental approaches based on dominant-inhibitory strategies have yielded contradictory results in regard to a role for Akt in insulin-stimulated glucose uptake, and not all studies have supported the kinase as important to insulin signaling in liver (*11–14*).

In rodents and humans, there are three Akt isoforms, each encoded by a separate gene (*15–17*). Because Akt2 appears to be enriched in insulin-responsive tissues and has been specifically implicated in the metabolic actions of the hormone (*18–20*), we generated mice with a targeted disruption in the *Akt2* locus by homologous recombination. The targeting vector was designed to insert *LoxP* sites (*21*) flanking the sequence containing


[1]Department of Biology, University of Pennsylvania, Philadelphia, PA 19104, USA. [2]Department of Medicine, [3]Department of Cell and Developmental Biology, [4]Department of Neuroscience, and [5]Department of Genetics, University of Pennsylvania School of Medicine, Philadelphia, PA 19104, USA. [6]Howard Hughes Medical Institute and the [7]Department of Internal Medicine, Yale University School of Medicine, New Haven, CT 06520, USA.

*To whom correspondence should be addressed. E-mail: birnbaum@mail.med.upenn.edu